

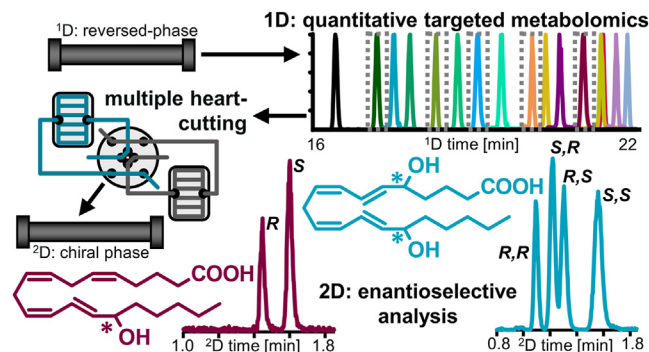
Deducing formation routes of oxylipins by quantitative multiple heart-cutting achiral-chiral 2D-LC-MS

Nadja Kampschulte[✉], Rebecca Kirchhoff[✉], Ariane Löwen[✉], and Nils Helge Schebb^{*✉}

Chair of Food Chemistry, School of Mathematics and Natural Sciences, University of Wuppertal, Wuppertal, Germany

Abstract Several oxylipins are regulators of inflammation. They are formed by enzymes such as lipoxygenases or cyclooxygenases, but also stereorandomly by autooxidation. Reversed-phase liquid chromatography-tandem-mass-spectrometry (LC-MS/MS) methods for oxylipin quantification do not separate enantiomers. Here, we combine sensitive and selective oxylipin analysis with chiral separation using two-dimensional (2D)-LC-MS/MS. By multiple heart-cutting, the oxylipin peaks are transferred onto a chiral column. 45 enantiomeric pairs of (di-)hydroxy-fatty acids are separated with full gradient elution within 1.80 min, yielding lower limits of quantification <1 pg on the column. Concentrations, as well as enantiomeric fractions of oxylipins, can be determined, even at low concentrations or at high enantiomeric excess of one isomer. The developed achiral-chiral multiple heart-cutting 2D-LC-MS/MS method offers unprecedented selectivity, enabling a better understanding of the formation routes of these lipid mediators. This is demonstrated by distinguishing the formation of hydroxy-fatty acids by (acetylated) cyclooxygenase-2 and radical-mediated autooxidation. Applying the method to human M2-like macrophages, we show that the so-called specialized pro-resolving mediators (SPM) 5,15-DiHEPE and 7,17-DiHDHA as well as 5,15-DiHETE were present as (*S,S*)-enantiomers, supporting their enzymatic formation. In contrast, at least eight isomers (including protectin DX but not neutroprotectin D1) of 10,17-DiHDHA are present in immune cells, indicating formation by autooxidation. In the human plasma of healthy individuals, none of these dihydroxy-fatty acids are present. However, we demonstrate that all four isomers quickly form via autooxidation if the samples are stored improperly. Dihydroxy-FA should only be reported as SPM, such as resolvin D5 or resolvin E4, if an enantioselective analysis as described here has been carried out.

Supplementary key words lipidomics • arachidonic acid • enantioselective analysis • autooxidation • enzymatic oxidation • lipid oxidation • resolvins • sample storage • lipoxygenase • cyclooxygenase



Oxylipins are a heterogeneous group of lipids derived from the oxidation of (poly-) unsaturated fatty acids. Several oxylipins are formed by non-enzymatic free radical reactions. The biosynthesis of oxylipins is catalyzed by lipoxygenases (LOX), cyclooxygenases (COX), or by cytochrome P450 monooxygenases (CYP). While the enzymatic pathways are highly stereo- and enantio-specific, the autooxidative pathways lead to stereorandom products (1, 2). Many oxylipins are potent lipid mediators that regulate physiological processes such as blood coagulation, fever, inflammation, and blood pressure. Liquid chromatography-tandem mass spectrometry (LC-MS/MS)-based multi-methods covering large numbers of structurally diverse oxylipins are state of the art for the investigation of lipid mediator biology (3–7). These powerful reversed-phase (RP) chromatography methods are characterized by high selectivity and sensitivity, which are achieved by narrow chromatographic peaks and selective MS/MS detection. They allow the separation and quantification of a large number of structurally similar oxylipins, including positional isomeric (di-) hydroxy-fatty acids (-FA). RP-based methods with achiral stationary phases do not enable the separation of oxylipin enantiomers. However, this is key for understanding the formation routes and biology of these compounds as

*For correspondence: Nils Helge Schebb, nils@schebb-web.de.

stereochemistry directs biological activity, receptor interactions, and metabolic fate (8–10).

Numerous chromatographic methods for enantioselective oxylipin analysis have been reported (10–15). However, most of these methods cover only a few oxylipins, except for a recent supercritical fluid chromatography- (SFC-) MS approach, which enables the quantification of a wide range of octadecanoids (16). Most commonly, amylose-based tris(3,5-dimethyl-phenylcarbamate) phases are employed for separating stereoisomeric oxylipins (10–12, 16–20). Under RP conditions, this material exhibits suitable stereoselectivity, yielding adequate retention as well as separation of stereoisomeric oxylipins such as hydroxy-FA enantiomers (10–12, 21). The chemical selectivity of this material for positionally isomeric oxylipins is limited, which leads to their poorer chromatographic resolution compared to RP chromatography (12, 20). Given that isobaric oxylipins, such as epoxy- and hydroxy-FA, show similar fragment spectra and share mass transitions, chiral chromatography shows insufficient specificity for structural isomers (10). Moreover, enantioselective chromatographic separation yields wider peaks compared to RP (ultra-high performance) LC and thus lower sensitivity. Therefore, the application of chiral chromatography for the comprehensive and quantitative analysis of oxylipins in biological samples is limited, and RP chromatography is the technique of choice for targeted oxylipin metabolomics (22).

Combining efficient RP chromatography and enantioselective separation is a promising approach for sensitive and selective but stereospecific analysis of oxylipins. This is possible by heart-cutting two-dimensional (2D) chromatography. Heart-cutting enables the transfer of selected sections or peaks of the ^1D chromatogram to a second column with orthogonal selectivity for further chromatographic separation. Achiral-chiral heart-cutting 2D-LC is frequently used for the analysis of amino acids (23, 24) or pharmaceuticals (25, 26). By loop-based *multiple* cutting, the collection of a large number of ^1D sections and subsequent ^2D analysis is possible (27). Despite its great potential, this approach has rarely been exploited for comprehensive targeted metabolomics.

In this work, an LC-MS/MS method was developed which enables the specific and enantioselective quantitative analysis of oxylipins. An efficient RP-LC separation was coupled with chiral chromatography in a 2D multiple heart-cutting (MHC) setup. Due to the efficient RP separation in the first dimension, positionally isomeric oxylipins and isobaric compounds are separated. Heart-cutting of the entire ^1D peak and efficient enantioselective separation by full-gradient elution on a chiral stationary phase enables sensitive and selective determination of a large number of oxylipin isomers, that is, ARA-, EPA-, DHA-, linoleic-, and linolenic acid-derived hydroxy- and dihydroxy-FA.

The method described here is one of the most comprehensive multiple heart-cutting applications reported thus far, and the first one for the analysis of oxylipins. This novel approach enables the elucidation of the formation pathways of oxylipins in biological samples based on quantitative oxylipin data and the ratio of the enantiomers with the same sensitivity and specificity as that of ID RP-LC-MS/MS.

MATERIALS AND METHODS

Instrumental analytical methods

Chromatographic separation was carried out with an Agilent 1290 Infinity II system (Agilent Technologies, Waldbronn, Germany). In the ID setup, the system comprises an autosampler, a binary pump, and a column oven. An established method for the analysis of more than 150 oxylipins was used in the first dimension (3). Solvent A is a mixture of water and solvent B (95/5) containing 0.1% acetic acid, and solvent B consists of acetonitrile, methanol, and acetic acid (800/150/1). The oxylipins are separated on a C18 reversed-phase column (Zorbax Eclipse Plus C18, 2.1 × 150 mm, particle size 1.8 μm , pore size 9.5 nm, Agilent Technologies) at 40°C with a flow rate of 0.3 ml/min and the following gradient: 21% B at 0 min, 21% B at 1.0 min, 26% B at 1.5 min, 51% B at 10 min, 66% B at 19 min, 98% B at 25.1 min, 98% B at 27.6 min, 21% B at 27.7 min, and 21% B at 31.5 min (3, 28). For detection, the LC was coupled to a Sciex 6500+ QTrap triple quadrupole mass spectrometer (AB Sciex, Darmstadt, Germany) operated in negative electrospray ionization (ESI(–)) mode. In quantitative ID analysis, the instrument was operated in scheduled multiple reaction monitoring (MRM), with ± 22 s windows around the expected retention time and a cycle time of 0.4 min. The ion source settings were as follows: Ionspray voltage: –4500 V, nebulizer gas (gas 1, zero air): 60 psi, drying gas (gas 2, zero air): 60 psi, temperature: 475°C, curtain gas (N_2): 35 psi. The collision gas (N_2) was set to 12 psi. The injection volume was 5 μl . The ID-LC and the MS were controlled using Analyst 1.7.3 Software (AB Sciex).

In the 2D setup, an additional binary pump, an additional oven, as well as a 2D heart-cutting valve with active solvent modulation (ASM, 1.9 μl ASM capillary, ASM factor 3), and two multiple heart-cutting decks with six 40 μl sample loops each were integrated into the system (Fig. 1). All heart cuts were triggered time-dependently based on the retention times of the oxylipins in the first dimension, which was determined prior to each 2D-LC batch (further details are described in the Supplemental Data). ^2D separation of the heart-cuts was carried out at 35°C on a short 50 × 3.0 mm Chiralpak IA-U column, ie, amylose tris(3,5-dimethylphenylcarbamate) material immobilized on 1.6 μm silica (Daicel, Osaka, Japan). Water with 10% acetonitrile and 0.1% acetic acid was used as solvent A, and acetonitrile with 10% water and 0.1% acetic acid was used as solvent B. A flow of 0.9 ml/min was applied (backpressure 300–400 bar). The ^2D gradient started with 5% B, which was kept for the duration of the ASM (0.14 min), and then increased to 45% B in 0.01 min. From 0.15 min to 1.40 min, the composition changed linearly to 70% B, which was held for 0.3 min, and subsequently, within 0.01 min, the initial conditions were restored and held for 0.09 min, yielding a ^2D cycle time of 1.80 min. An idle flow rate of 0.4 ml/min was used before and between the individual ^2D runs. Mass spectrometric detection was carried out in negative MRM, with a

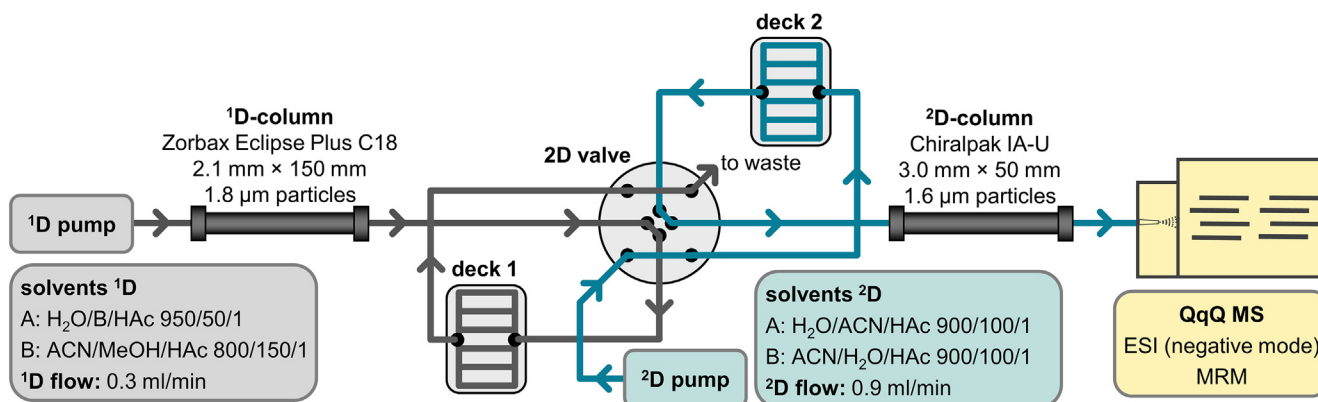


Fig. 1. Setup of the multiple heart-cutting 2D-LC system. Gradient separation in the first dimension is carried out with an C18 stationary phase. The 2D valve directs the eluate of the first dimension to the parking decks. Each deck hosts six capillaries with a volume of 40 μ l which serve as sample loop for the 2 D analysis. Gradient chiral separation in the second dimension is carried out with an amylose-based tris(3,5-dimethyl-phenylcarbamate) phase in reversed-phase mode. The oxylipins are detected by MS/MS.

dwel time of 12 ms for each transition. The following parameters of the ion source were adapted to the higher solvent flow: gas 2: 70 psi, temperature: 600°C, curtain gas: 40 psi. The 2D-LC system was controlled using OpenLab CDS ChemStation Edition (C.01.10.) software (Agilent), and the mass spectrometer was controlled using Analyst 1.7.3 Software (AB Sciex). Chromatographic resolution R of two peaks was calculated as $R = 1.18 \cdot \frac{t_{R2} - t_{R1}}{FWHM_1 + FWHM_2}$, whereas t_{R1} and t_{R2} are the retention times of the earlier and later eluting peaks, respectively, and FWHM are the full peak widths at half height.

Cell culture, plasma generation, enzymatic reactions, and oxylipin extraction

2×10^6 HCA-7 cells were cultivated in 60 cm^2 dishes for 24 h (29). *Tert*-butyl hydroperoxide (tBuOOH) or COX inhibitors were added into the medium, and after 3 h (tBuOOH) or 24 h (COX inhibitors) the cells were harvested using trypsin and sonicated in a mixture of water and methanol (50/50) containing an antioxidant solution (30). M2-like primary human macrophages were generated and cultivated as previously described (3, 31).

Pooled human EDTA plasma and pooled human serum from healthy individuals were generated as described (2), approved by the ethics committee of the University of Wuppertal and in accordance with the guidelines of the Declaration of Helsinki. In brief, for plasma generation, blood was collected in EDTA-monovettes and immediately centrifuged for 10 min at 1200 g and 4°C. The supernatant was carefully collected. Plasma samples from different subjects were pooled, gently mixed, aliquoted, and frozen at -80°C immediately afterward. Of note, plasma and serum were obtained from different donors. In addition, citrate plasma from four individuals, which was stored at -40°C for several months, was provided by the blood donation center at University Hospital Düsseldorf (Düsseldorf, Germany). Commercial human pooled EDTA plasma was purchased from BioIVT (West Sussex, United Kingdom), which showed high concentrations of lipid autoxidation products presumably resulting from processing and storing in a non-frozen state for an extended period (oxidized plasma).

For 15-LOX-catalyzed conversion of 5(*R,S*)-HETE, 5(*R,S*)-HEPE, and 4(*R,S*)-HDHA, 5 μM of the compounds were incubated with a homogenate of stably transfected HEK293T

cells inducibly expressing *ALOX15* (30) for 15 min (Supplemental Data). Enantioselective depletion of one stereoisomer from a racemic mixture was performed by Amano-Lipase PS-catalyzed transesterification (Supplemental Data) (32). The autoxidation of human plasma was induced by storing plasma in a non-light-protected environment at 20°C – 23°C for up to seven days. The extraction of non-esterified oxylipins from plasma, serum, and cell homogenates was carried out by solid-phase extraction on a non-polar C8/strong anion exchange mixed-mode material (Bond Elut Certify II, 200 mg, Agilent Technologies) as described (28, 33). Details of the origin of the used chemicals and biological materials are provided in the Supplemental Data.

RESULTS

In order to enable both, sensitive and selective quantification of oxylipins and specific determination of enantiomeric ratios, we developed the first 2D targeted oxylipin metabolomics platform: By multiple heart-cutting (MHC), the oxylipins are collected from the first (RP) dimension and injected into the second dimension, where chiral separation is performed (Fig. 1). By separating and isolating isobaric compounds and positional isomers in the first (RP) dimension, interferences in the chiral separation are minimized.

Quantitative 1D oxylipin metabolomics

The 1D setup is based on a well-established targeted LC-MS/MS lipidomics method covering 239 oxylipins. Quantification of oxylipins is performed via an external calibration using authentic reference standards with 29 isotopically labeled oxylipins as internal standards (supplemental Table S2–S3) (3, 34). Using this method, hydroxy- and vicinal dihydroxy-FA elute as narrow peaks with full peak widths at half height (FWHM) of 4–5 s over a broad window from 13 min to 22 min, ensuring an efficient chromatographic separation (Table 1) (3, 28, 33, 34). This is crucial because several critical separation pairs, ie, isobaric compounds giving rise to similar fragment spectra, need to be chromatographically separated prior

TABLE 1. Separation and MS detection parameters of the enantioselective multiple heart-cutting 2D-LC method

Analyte	m/z Q1	m/z Q3	DP [V]	CE [V]	ID LLOQ		^1D tR [min] ^b	Peak 1		Peak 2		Resolution ^d
					[nM] ^a	[pg on column] ^a		^2D tR [min] ^c	^2D FWHM [s]	^2D tR [min] ^c	^2D FWHM [s]	
9-HODE ^e	295.2	171.1	-80	-26	0.14	0.21	20.31	1.646	1.82	1.939	2.30	5.04
13-HODE ^e	295.2	195.2	-80	-26	0.25	0.37	20.20	1.547	1.66	2.001	2.21	8.30
9-HOTrE	293.2	171.2	-65	-22	0.50	0.74	17.68	1.565	1.75	1.733	2.06	3.13
13-HOTrE	293.2	195.1	-70	-24	2.5	3.7	18.08	1.326	1.45	1.535	1.82	4.53
13- γ -HOTrE	293.0	193.0	-70	-25	5.0	7.4	18.43	1.025	1.57	1.218	1.78	4.08
5-HETE	319.2	115.2	-60	-21	0.18	0.29	22.30	1.430	1.73	1.525	2.03	1.78
8-HETE	319.2	155.2	-60	-22	0.94	1.5	21.76	1.434	1.82	1.555	1.98	2.26
9-HETE	319.2	167.2	-60	-23	1.33	2.1	22.07	1.429	1.60	1.487	1.59	1.29
11-HETE	319.2	167.2	-60	-23	0.11	0.18	21.44	1.411	1.62	1.514	1.77	2.17
12-HETE	319.2	179.2	-60	-20	0.25	0.40	21.80	1.527	1.80	1.606	2.06	1.44
15-HETE	319.2	219.2	-60	-20	2.2	3.5	20.94	1.455	1.91	1.610	2.05	2.77
16-HETE	319.2	233.1	-65	-20	0.75	1.2	19.76	1.318	1.82	1.477	1.81	3.10
5-HEPE	317.2	115.1	-60	-20	0.30	0.48	19.96	1.282	1.78	1.345	1.95	1.19
8-HEPE	317.2	155.2	-60	-20	0.30	0.48	19.23	1.258	1.66	1.344	1.84	1.73
9-HEPE	317.2	167.0	-40	-19	0.50	0.80	19.61	1.248	1.49	1.307	1.74	1.30
11-HEPE	317.2	167.0	-40	-21	0.31	0.49	19.01	1.294	1.59	1.371	1.85	1.57
12-HEPE	317.2	179.2	-65	-20	0.50	0.80	19.44	1.343	1.59	1.420	1.77	1.61
15-HEPE	317.2	219.2	-60	-20	0.75	1.2	18.90	1.281	1.74	1.336	1.78	1.12
18-HEPE	317.2	259.2	-55	-17	0.75	1.2	18.15	1.249	1.47	1.288	1.57	0.85
4-HDHA	343.2	101.1	-55	-19	0.25	0.43	22.72	1.401	1.60	1.488	1.73	1.86
7-HDHA	343.2	141.2	-55	-19	0.50	0.86	21.97	1.395	1.58	1.455	1.71	1.31
8-HDHA	343.2	189.2	-50	-19	0.29	0.50	22.15	1.376	1.70	1.414	1.87	0.74
10-HDHA	343.2	153.2	-45	-21	0.25	0.43	21.59	1.413	1.62	1.499	1.77	1.79
11-HDHA	343.2	121.1	-45	-20	0.25	0.43	21.86	1.417	1.63	1.470	1.65	1.13
13-HDHA	343.2	193.2	-55	-19	0.25	0.43	21.37	1.433	1.73	1.532	1.72	2.03
14-HDHA	343.2	205.2	-50	-19	0.41	0.71	21.59	1.422	1.63	1.493	1.81	1.46
16-HDHA	343.2	233.2	-55	-19	0.25	0.43	21.10	1.420	1.68	1.469	1.75	1.01
17-HDHA	343.2	201.2	-60	-20	8.5	15	21.21	1.408	1.65	1.460	1.62	1.13
20-HDHA	343.2	241.2	-55	-19	0.50	0.86	20.59	1.344	1.57	1.383	1.61	0.88

Shown are the MRM transitions and the MS parameters (declustering potential, DP and collision energy, CE) used for detection, the lower limit of quantification (LLOQ) in the first dimension, retention times, peak width (full width at half-maximal height, FWHM), and chromatographic resolution between the enantiomers.

^aThe lower limit of quantification (LLOQ) was set to the lowest calibration standards with a signal-to-noise ratio ≥ 5 and an accuracy $100 \pm 20\%$.

^bRelative standard deviation of the ^1D retention times within one batch was $<0.1\%$ (0.01 min) and $<0.3\%$ (0.06 min) across different batches.

^cRelative standard deviation of the ^2D retention times within one batch was $<0.3\%$ (0.005 min) and $<1\%$ (0.02 min) across different batches.

^dChromatographic resolution between the enantiomers was calculated as the ratio between the difference in the retention times and the sum of the FWHM of two peaks, multiplied by 1.18.

^eA longer gradient up to 85% B was used due to the strong retention of these LA-derived oxylipins on the 2D column.

to MS/MS detection. Well-known examples of such pairs are hydroxy-FA and their corresponding epoxy derivatives (eg, 15-HETE and 14(15)-EpETrE) (10). However, this is also the case for several hydroxy-FA: For example, 7-HDHA shows a signal on the transition of 17-HDHA, 9- and 11-HEPE share characteristic fragments, as well as 9-HETE with 11-HETE and 12-HETE (supplemental Fig. S1).

Enantioselective ^2D analysis of oxylipins

Chiral separation of oxylipins was carried out on a short (50 mm) column with $< 2 \mu\text{m}$ particles. The amylose-based tris(3,5-dimethyl-phenylcarbamate) material yields good selectivity and allows the application of reversed-phase conditions. Active solvent modulation was used during the transfer of the heart-cuts to the ^2D column because this improved the retention and separation of the enantiomers (Supplemental Data). Due to the short column, a rapid (1.80 min total ^2D run time) linear gradient of water and acetonitrile with 0.1%

acetic acid could be used, which led to efficient separation of the enantiomers of hydroxy- and vicinal dihydroxy-FA (Table 1, supplemental Table S5). An addition of methanol or isopropanol to the solvents did not improve the separation (supplemental Table S4), although earlier reports showed clear changes in the selectivity for the separation of hydroxy-FA when different alcohols are used with the same stationary phase under normal-phase conditions (18, 35).

For the 2D interface, sample loops for MHC with a volume of 40 μl were selected. This corresponds to 0.12–0.14 min of the ^1D gradient and the full width at 10% peak height (FWTM) of the ^1D peaks. The FWTM interval equals more than 96% of a Gaussian peak. Thus, practically the entire ^1D peak is transferred to the second dimension without losing relevant amounts of the eluting oxylipin (Fig. 2A). At the same time, the transfer window is equally narrow as the ^1D peaks, preserving the separation and thus specificity of the first dimension.

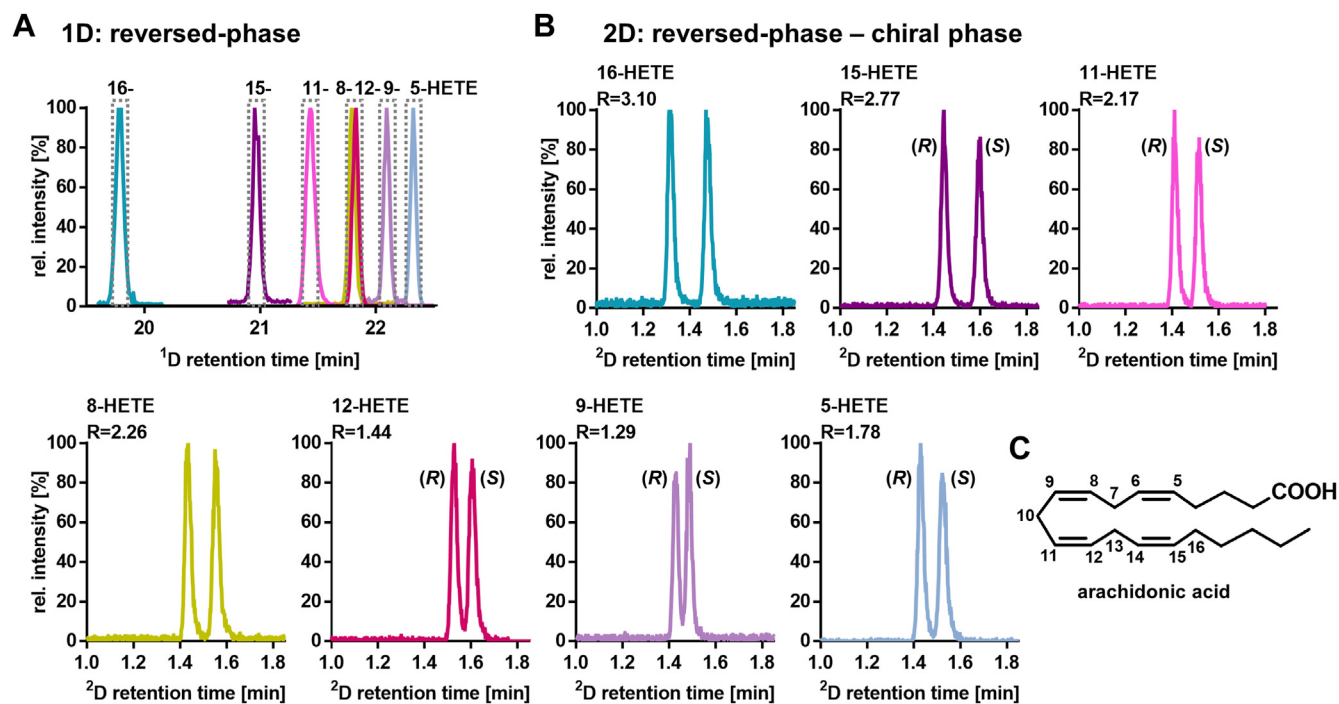


Fig. 2. Chiral separation of arachidonic acid-derived oxylipins by means of 2D-LC-MS/MS. A: ¹D chromatogram using a RP-18 stationary phase (2.1 mm × 150 mm, 1.8 μm particles) and acidified water and acetonitrile with methanol as solvents. The dashed lines indicate the volume that is collected in the ²D sample loop. B: Multiple heart-cut ²D chromatograms following chiral separation using an amylose-based tris(3,5-dimethyl-phenylcarbamate) phase (3.0 mm × 50 mm, < 2 μm particles) and acidified water and acetonitrile as eluents. Detection in both, 1D- and 2D-LC was carried out by a triple quadrupole MS in MRM following electrospray ionization in negative mode. The separation of a racemic multi-analyte oxylipin standard (50 nM) is shown. The *R* and *S* isomers are indicated for the peaks of the enantiomeric pairs, when stereo information could be deduced with enantiomerically pure standards or by enzymatic depletion of one enantiomer. C: Chemical structure of arachidonic acid with atom numbering indicating the positions of the hydroxy groups.

Heart-cutting can be triggered at any time point, and thus, it is possible to transfer every peak from the first dimension into the ²D sample loop and subsequently further resolve it with the orthogonal selectivity in the second dimension. Thus, practically, the number of oxylipins that can be chirally separated in the second dimension in an individual analysis run is limited by the number of available loops in the 2D decks. Due to the rapid ²D gradient (1.80 min) and the “smart peak parking” feature of the 2D-LC software, 12 to 15 heart-cuts can be collected within the runtime of the first dimension (32 min), resulting in a total runtime of 32–45 min. Due to the co-elution of non-isobaric compounds (Table 1) this allows the chiral analysis of up to 20 oxylipins (An exemplary sampling table is provided in the supplemental Table S1). This is in our hands sufficient for addressing biological questions. Consistently, previous published chiral methods cover a similar number of oxylipins, eg, 16 pairs of enantiomers (10), a total of 37 lipid mediators (11) or 19 enantiomeric pairs along with two diastereomeric compounds (12). However, if the enantiomeric fraction of all 45 oxylipins covered by the 2D method should be analyzed, at least two injections are necessary.

With 1.80 min, the duration of the ²D gradient of this method is shorter in comparison to other MHC applications, where ²D chromatography with gradient

elution is carried out in five minutes for the characterization of synthetic oligonucleotides (36), in two minutes for determining additives in polystyrene (27) or within nine minutes for analyzing pyrrolizidine alkaloids in plants (37). For the enantioselective separation of amino acids, a considerably faster ²D separation of 68 s is described (24). However, an isocratic separation was used in this study. This is common for achiral-chiral (multiple) heart-cutting methods, but not applicable to the structurally diverse class of oxylipins. Other 2D methods with a chiral second dimension aim to analyze individual heart cuts, using ²D runtimes from four (23), six (25), or seven minutes (26) up to more than 30 min (38), which is not suitable for multiple heart-cutting methods.

The efficient chromatography in the second dimension yields full peak widths at half height (FWHM) < 2.5 s for most of the oxylipin isomers (Table 1). This is in line with other chiral MHC 2D approaches, eg, for the analysis of amino acids (FWHM ~2–4 s) (24), and slightly narrower in comparison to a chiral 1D method in which the same < 2 μm packing is used as the enantioselective stationary phase for the separation of oxylipins (FWHM ~3 s) (12). However, all other methods describing the enantioselective analysis of oxylipins have reported considerably wider peaks (FWHM ~9 s) (10, 11).

With the rapid generic ^2D gradient, the separation of 29 enantiomeric hydroxy-FA is achieved (Table 1): Seven ARA-derived hydroxy-FA enantiomers (HETE) are separated at baseline (Fig. 2). Furthermore, ten pairs of stereoisomeric DHA- and seven EPA-derived hydroxy-FA (HDHA and HEPE, respectively) can be separated, as well as five hydroxy-octadecanoids from linoleic and linolenic acid (Table 1, supplemental Fig. S4).

Of note, the developed method also includes the chiral analysis of 16 vicinal *threo*-dihydroxy-FA (Supplemental Data). With this performance, separating > 40 pairs of oxylipin enantiomers, the described MHC-2D method is the most comprehensive platform for the enantioselective analysis of oxylipins so far: There are established methods covering specific sets of oxylipins, e.g., ARA-derived hydroxy-FA (13, 19, 20) or the major oxidation products of ARA, EPA, and DHA of the LOX- and COX-branches of the ARA cascade (11, 39). With few methods, a comprehensive set of HETE-isomers, selected HEPE and HDHA together with PGE- and PGD-species (12) or with epoxy-FA (10) is analyzed. However, none of these methods provides a comparable comprehensive insight into the ARA cascade, allowing a quantitative analysis together with the determination of the enantiomer ratio as the MHC-2D-LC-MS/MS platform presented here.

DISCUSSION

Determination of enantiomeric fractions

With the developed platform, the quantitative analysis of oxylipins is extended by another important yet rarely addressed parameter: the ratio of enantiomers, expressed as the enantiomeric fraction (EF), ie, the proportion of one enantiomer in the sum of all ($EF = \frac{\text{peak area 1}}{\text{peak area 1} + \text{peak area 2}}$), which is slightly different from the earlier used enantiomeric excess ($ee = \frac{\text{peak area 1} - \text{peak area 2}}{\text{peak area 1} + \text{peak area 2}}$) (40). Quantitative analysis and determination of EF are carried out in two individual runs. Quantification using 1D chiral methods is complicated because of the limited availability of corresponding isomerically pure standards and the even more limited availability of deuterated analogs. The determination of the EF in the heart cut by chiral separation in the second dimension does not require enantiomerically pure and isotope-labeled standards: The enantiomeric ratio can be directly calculated from the MRM peak area ratio of the enantiomers. Neither the extraction of oxylipins from biological samples (34, 41) nor RP chromatography or heart-cutting and transfer discriminate one of the enantiomers. They show the exact same MS/MS behavior, and as the solvent composition of the two peaks differs in the gradient by less than 10%, the ionization efficiency is not affected (42). Also, ion suppression is unlikely because, on the one hand, the interfering matrix is strongly reduced by the SPE-based sample preparation (43) and on the other hand, only a small fraction of the ^1D run is transferred to the second

dimension. Thus, these systematic method errors do not influence the determined EF. Most importantly, unlike previously available enantioselective one-dimensional methods for oxylipins, there is no risk of interference from isobaric molecules. These are either chromatographically separated in the first dimension or can be selectively detected without interference by specific mass transitions. Thus, following absolute quantification of the oxylipin by means of 1D-RP-LC-MS/MS, the ratios of the enantiomers can be determined reliably and precisely by MHC-2D-LC-MS/MS.

Even for only partially resolved isomers, the enantiomeric ratio can be quantified even at a high enantiomeric excess, for example, for 18(*R*)-HEPE and 18(*S*)-HEPE ($R = 0.85$, Fig. 3A). If the concentrations of both enantiomers exceed the quantification limit, the EF can reliably be determined up to a ratio of 10%:90%.

Due to the narrow peaks in both dimensions and the optimized loop size for the heart cut, the entire ^1D peak is transferred to the second dimension. As a result, the sensitivity of the ^2D enantioselective method is comparable to the highly sensitive 1D quantitative targeted metabolomics method: For example, defining peaks with a signal-to-noise ratio ($S/N \geq 3$) as the limit of detection, 0.80 pg of 18-HEPE can be detected by means of 1D-LC-MS/MS. The same S/N is achieved following MHC-2D-LC-MS/MS of 0.80 pg of each 18-HEPE enantiomer (Fig. 3B). For quantitative analyses, the lower limit of quantification (LLOQ) is defined by a $S/N \geq 5$ and an accuracy of $100 \pm 20\%$ within the calibration curve (https://www.ema.europa.eu/en/documents/scientific-guideline/ich-guideline-m10-bioanalytical-method-validation-step-5_en.pdf). This value is typically 1.5–2.5 times higher than the LOD. Also regarding the LOQ, the performance of the two-dimensional method is comparable to that of the one-dimensional one (supplemental Fig. S3). Thus, the 2D method is more or equally sensitive as other less comprehensive enantioselective methods for the determination of oxylipins (10–13).

To evaluate the precision of the developed methodology, oxylipin concentrations, and their EF were determined in three different sample types of human plasma and serum on three different days. The high precision (<15% relative standard deviation (RSD)) of quantitative oxylipin analysis in plasma and serum within and across different days (supplemental Table S6) fulfills the criteria of international guidelines (https://www.ema.europa.eu/en/documents/scientific-guideline/ich-guideline-m10-bioanalytical-method-validation-step-5_en.pdf) and is comparable to or better than other targeted oxylipin methods (11, 12, 28, 33). The determination of the EF by MHC-2D-LC-MS/MS yields even more precise results: RSD of less than 5% in the inter-day comparison were observed, and except for few oxylipins on individual days, the method yields high intra-day precision with an RSD < 10% (supplemental Table S6).

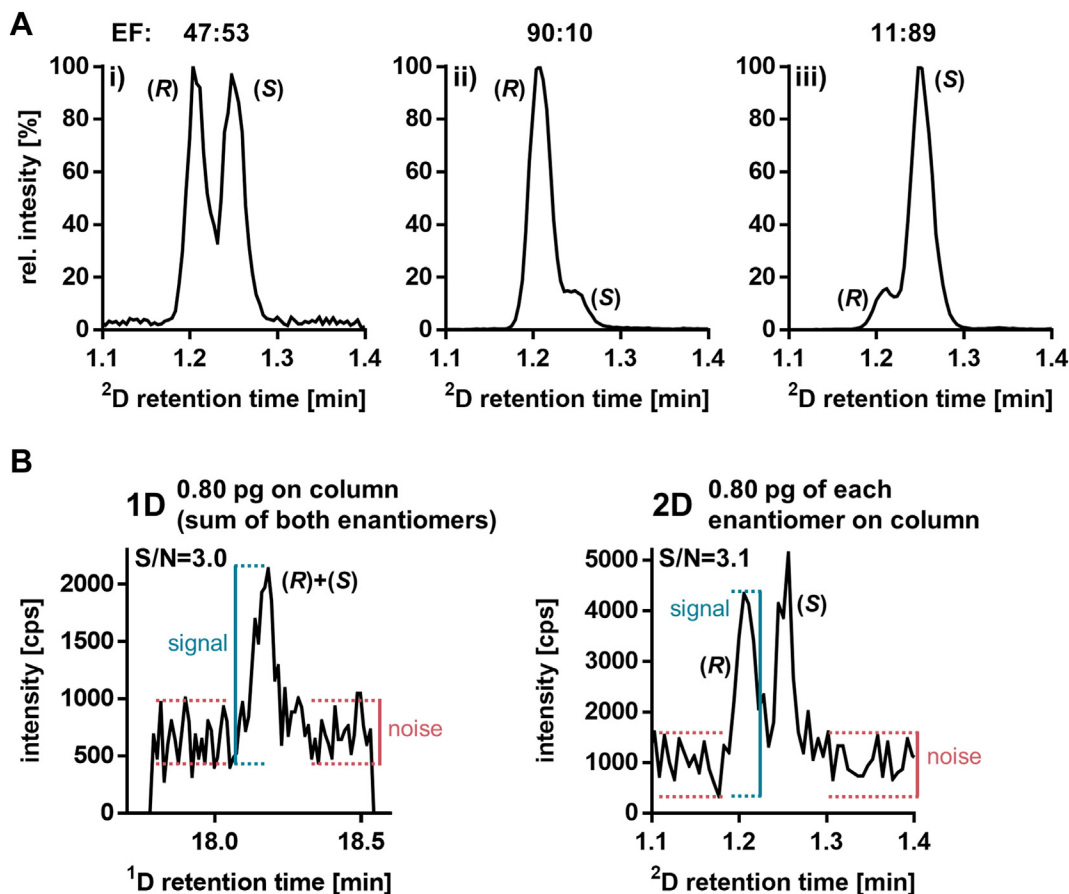


Fig. 3. Determination of the enantiomeric fraction (EF) and detection limit of non-baseline separated 18-HEPE. A: Achiral – chiral ^2D chromatograms of (i) a racemic mixture of 18-HEPE, (ii) 18-(*R*)-HEPE along with a small amount of 18-(*S*)-HEPE and (iii) 18-(*R*)-HEPE with a large excess of 18-(*S*)-HEPE. B: LC-ESI(–)-MS/MS chromatogram of an injection of a 0.5 nM racemic 18-HEPE standard (0.80 pg on column) measured by 1D reversed-phase chromatography (left) and ^2D chromatogram following heart-cutting and chiral separation (right) of a 1 nM racemic 18-HEPE standard (1.6 pg total, ie 0.80 pg of each enantiomer on column). In the chromatograms, the determination of the signal-to-noise ratio (S/N) is illustrated, showing the (S/N) ≥ 3 defined as limit of detection.

Enantioselective analysis of hydroxy-fatty acids

To demonstrate the applicability of the MHC-2D-LC-MS/MS method, the enzymatic and autooxidative formation of hydroxy-FA and the modulation of these pathways were analyzed in HCA-7 cells. This human colon carcinoma cell line overexpresses *PTGS2*, the cyclooxygenase-2 (COX-2)-coding gene, resulting in a high abundance of the COX-2 (44). Treatment of this cell line with the irreversible COX inhibitor acetylsalicylic acid (ASA) or the non-competitive selective COX-2 inhibitor celecoxib decreased the concentration of oxylipins resulting from COX-2 activity, such as PGE_2 and 12-HHTrE (supplemental Fig. S5), and the side product 11-HETE (Fig. 4A). MHC-2D-LC-MS/MS revealed the predominant formation of 11(*R*)-HETE, and stereoisomerism was not affected by ASA or celecoxib (Fig. 4A and D). Incubation with celecoxib also reduced 15-HETE levels in the cells without affecting the EF. However, following ASA treatment of HCA-7 cells, increased 15-HETE formation was observed (Fig. 4B). While non-treated as well as celecoxib-treated cells showed an excess of 15(*S*)-HETE (EF: 80%), ASA

incubation yields almost enantiopure formation of 15(*R*)-HETE (EF: 92%) (Fig. 4B and E). These findings are consistent with the reported peroxidase activity of COX, by which 11(*R*)-H(p)ETE and 15(*S*)-H(p)ETE are formed as side products (45), and with the finding that COX inhibition with ASA leads to an increase in 15-HETE formation (46). Mechanistically, the inhibition of COX-2 by ASA results from the acetylation of Ser516 in the active site of the enzyme. However, this modification of the enzyme does not inhibit the COX-2-catalyzed formation of 15-HETE but changes the stereospecificity of the reaction towards 15(*R*)-HETE (47).

Consistent with the absence of 5-LOX in this colon cell line (48), low levels of almost racemic 5-HETE are found under basal conditions, indicating non-enzymatic formation. The incubation of the cells with the oxidative stress-causing agent *tert*-butyl hydroperoxide (*t*BuOOH) increased the level of 5-HETE (Fig. 4C and F). The EF of 5(*R*)- and 5(*S*)-HETE do not change following *t*BuOOH treatment, as this agent induces (stereorandom) non-enzymatic lipid (per-)oxidation (Fig. 4C and F).

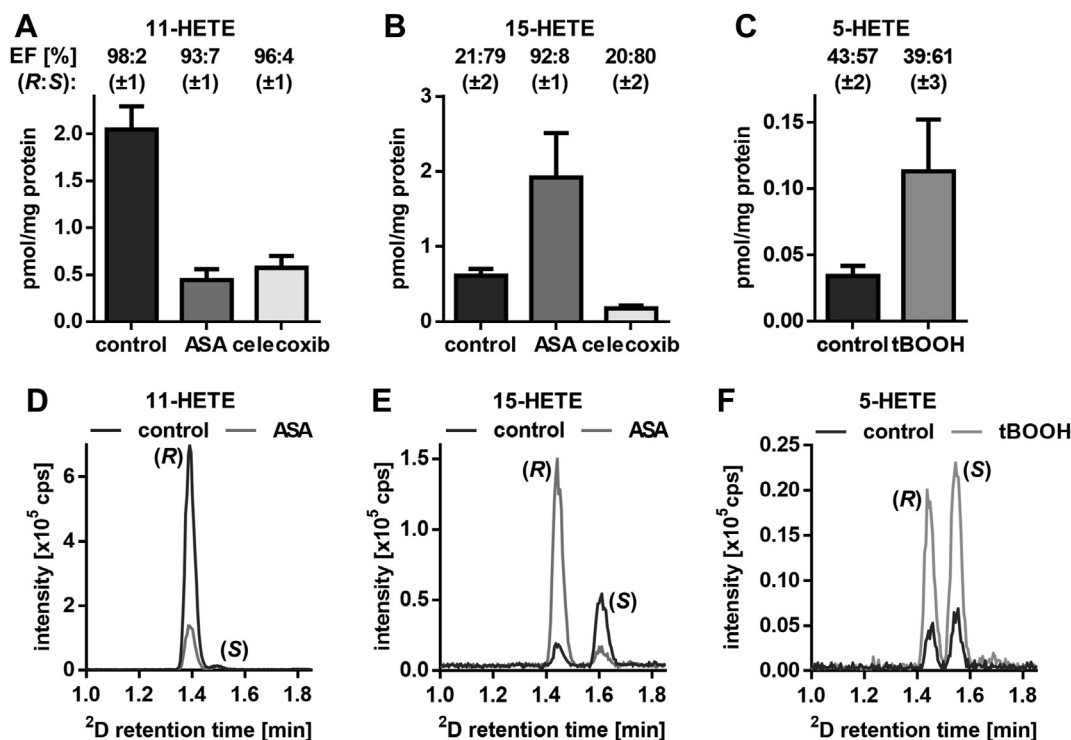


Fig. 4. Enzymatic and non-enzymatic formation of hydroxy-fatty acids in cell culture. COX-2 expressing HCA-7 cells were incubated with 100 μ M acetylsalicylic acid (ASA) for 24 h, 10 μ M celecoxib for 24 h or 100 μ M *tert*-butyl hydroperoxide (tBOOH) for 3 h. A: inhibition of COX-2-catalyzed 11-HETE formation by ASA and celecoxib. B: inhibition of COX-2-catalyzed 15-HETE formation by celecoxib and 15(*R*)-HETE formation by ASA-acetylated COX-2. C: *tert*-Butyl hydroperoxide-induced increase of 5-HETE concentrations. D: ²D-MRM chromatogram of 11-HETE, indicating the COX-2-catalyzed formation of 11(*R*)-HETE, which is inhibited by ASA. E: ²D-MRM chromatogram of 15-HETE, indicating the increased formation of 15(*R*)-HETE by ASA-acetylated COX-2. F: ²D-MRM chromatogram of 5-HETE indicating racemic formation of 5(*R,S*)-HETE by non-enzymatic oxidation induced by tBOOH.

Hydroxy-FA can be formed by autoxidation in plasma. Consistent with earlier reports (34) we show that prolonged storage of plasma at room temperature leads to an increase in the concentrations of hydroxy-fatty acids (shown for 5-HETE, 12-HETE and 15-HETE in supplemental Fig. S6). Both enantiomers of the respective hydroxy-FA are found in the improperly stored plasma samples in almost equal amounts, underlining the formation by autoxidation. An increase in hydroxy-FA levels in plasma has also been described at lower temperatures (−20°C) after a period of 6–12 months (49).

Analyzing commercial plasma, supraphysiological high levels of oxylipins are found (supplemental Table S6). The EF of 50%:50% of the enantiomers of the hydroxy-FA, including 12-HETE, indicates an autoxidative origin of these oxylipins (supplemental Table S6), presumably formed during inappropriate storage and/or plasma preparation. Only for the vicinal dihydroxy-FA 14,15-DiHETrE formed by hydrolysis of CYP-derived 14(15)-EpETrE (50) concentrations similar to those in freshly prepared plasma and serum are found in the commercial (oxidized) plasma, with a clear excess of one enantiomer (EF 16%:84%) (supplemental Table S6).

In well-prepared and stored plasma, the concentrations of hydroxy-FA are lower than in the oxidized one, and those oxylipins which are canonical products of human lipoxygenases, for example, 5-HETE, 12-HETE, and 15-HETE, show an excess of one enantiomer (EF > 60%) (supplemental Table S6). Consistent with the activation of platelets, 12-HETE, a downstream product of platelet-derived 12-LOX (51), is dramatically (~150 fold) increased in serum compared with plasma, with a massive excess of 12(*S*)-HETE (EF: 99.7%) (supplemental Table S6).

Formation of dihydroxy-fatty acids in plasma and primary human macrophages

Multiple hydroxy-fatty acids – several are referred to as specialized pro-resolving mediators (SPM) – are discussed to exhibit potent physiological effects in the regulation of inflammatory processes. However, the signaling (48, 52), occurrence (33, 48), and formation routes (48, 53–55) of these compounds are largely unclear. Trihydroxy-fatty acids are not reliably detectable in biological samples (33, 48) such as leucocytes (53). Several dihydroxy-fatty acids have been consistently reported in macrophages (53), but their occurrence in plasma is controversial (33, 48, 49, 56, 57). The

dihydroxy-FA 5,15-DiHEPE, 5,15-DiHETE, and 7,17-DiHDHA are not detected in carefully collected and well-prepared serum or plasma from healthy human subjects (Fig. 5). Only marginal concentrations of 5,15-DiHETE are present in citrate plasma that has been stored at -40°C for several months (Fig. 5E). However, when the plasma is (inappropriately) stored at room temperature for a few hours or up to several days, a rapid increase in dihydroxy-FA concentrations is observed (Fig. 5). High amounts are also found in the (oxidized) commercial plasma (Fig. 6, supplemental Fig. S8). This is consistent with the earlier report showing that 5,15-DiHETE concentrations increase after 6 months even if plasma is stored in a frozen state (-20°C) (49). This indicates that a major portion, if not all 5,15-DiHEPE, 5,15-DiHETE, and 7,17-DiHDHA reported in plasma, is formed artificially during sample preparation or storage. In studies that aim to correlate the concentrations of these oxylipins in plasma with biological effects, the formation route of these compounds has to be characterized.

For this purpose, the MHC-2D-LC-MS/MS method was applied to these dihydroxy-fatty acids. As expected, the enantiopure synthetic standards of 5(*S*),15(*S*)-DiHETE, 5(*S*),15(*S*)-DiHEPE (resolvin E4), as well as 7(*S*),17(*S*)-DiHDHA (resolvin D5) showed only one peak in both, ^1D (Fig. 6A) and ^2D (Fig. 6B) chromatograms. By the enantioselective conversion of racemic 5-HETE, 5-HEPE, and 7-HDHA by human 15-LOX (only giving rise to (*S*)-hydro(pero)xy-FA (58)), the diastereomeric pairs 5(*R*),15(*S*)- and 5(*S*),15(*S*)-DiHETE, 5(*R*),15(*S*)- and 5(*S*),15(*S*)-DiHEPE as well as 7(*R*),17(*S*)- and 7(*S*),17(*S*)-DiHDHA were generated. Chromatographic separation of these diastereomers was not possible by 1D RP chromatography (Fig. 6A). Coelution of these diastereomers was also found on other RP materials (supplemental Fig. S7), although several diastereomeric oxylipins can be effectively separated by RP chromatography, for example, 7(*R*),14(*S*)- and 7(*S*),14(*S*)-dihydroxy-4(*Z*),8(*E*),10(*E*),12(*Z*),16(*Z*),19(*Z*)-DHA (maresin 1 and 7(*S*)-maresin 1) (33), as well as 10(*S*),17(*S*)-dihydroxy-4(*Z*),7(*Z*),11(*E*),13(*Z*),15(*E*),19(*Z*)-

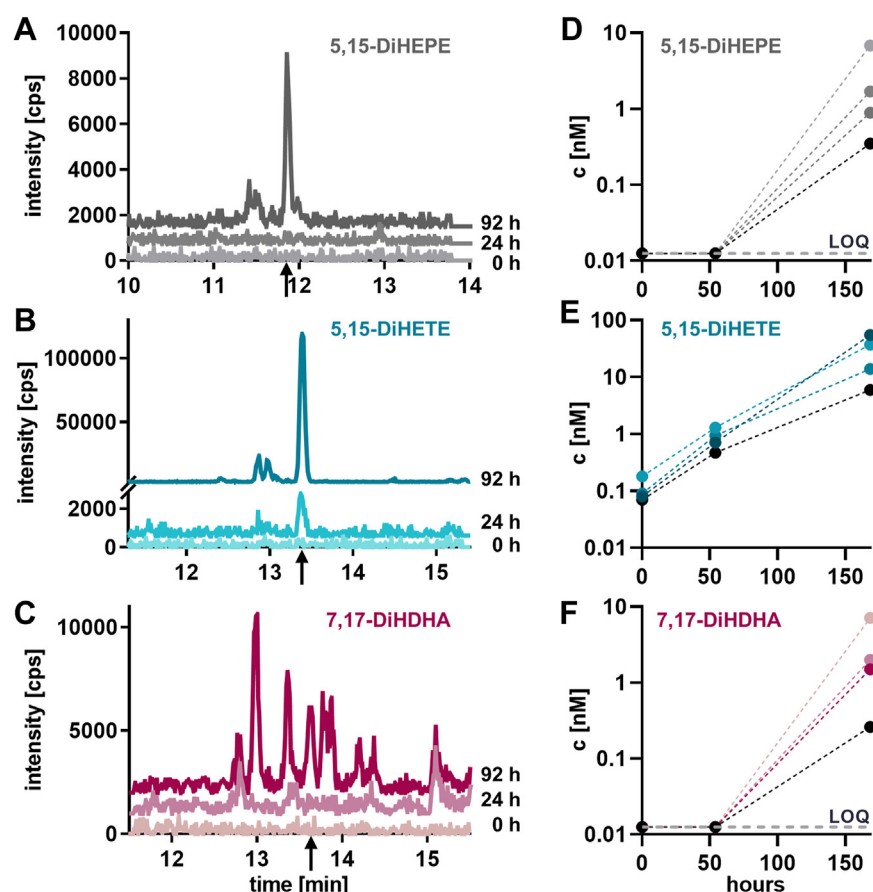


Fig. 5. Formation of dihydroxy-FA in human plasma during storage at room temperature. A–C: ID RP chromatograms (MRM signals) of the analysis of pooled EDTA plasma at baseline (0 h) and after storage for 24 h and 92 h. The arrows indicate the retention time of the (A) 5,15-DiHEPE, (B) 5,15-DiHETE, and (C) 7,17-DiHDHA. The signals after 24 h and 92 h are shown with an offset of 600–2800 cps. Chiral 2D analysis of the peaks of 15-DiHETE, 5,15-DiHEPE, and 7,17-DiHDHA unveiled peaks of all isomers, similar to that of oxidized plasma (Fig. 6). D–E: time-dependent formation of (D) 5,15-DiHEPE, (E) 5,15-DiHETE, and (F) 7,17-DiHDHA in citrate plasma of four human subjects. The following MRM transitions were used: 5,15-DiHETE: m/z 335→173; 5,15-DiHEPE: m/z 333→173; 7,17-DiHDHA: m/z 359→141.

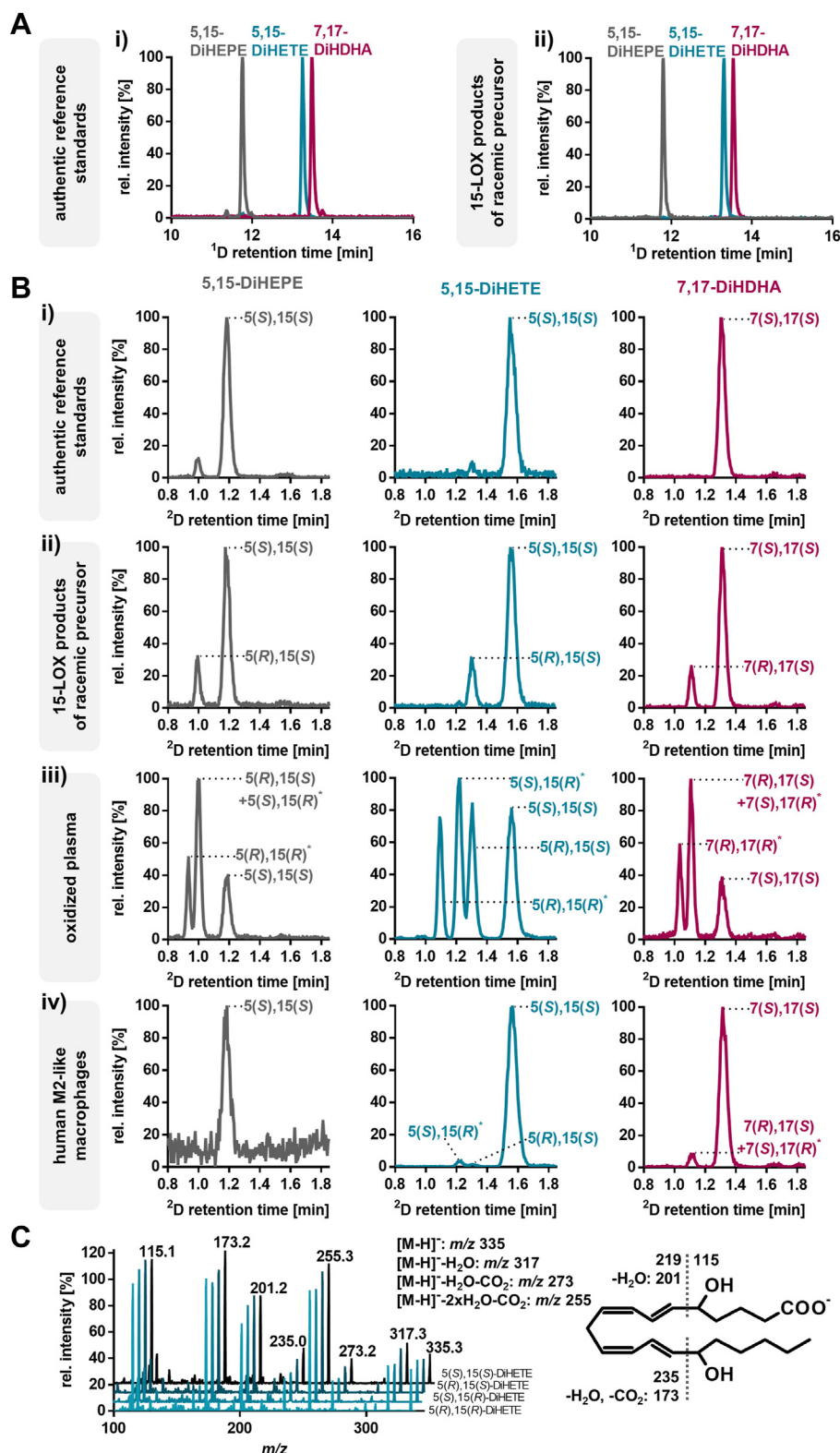


Fig. 6. Analysis of dihydroxy-ARA, EPA and DHA in plasma and cells by enantioselective heart-cutting 2D-LC. **A:** RP chromatograms (MRM signals) of (i) a standard mixture (50 nM) containing 5(*S*),15(*S*)-DiHETE, 5(*S*),15(*S*)-DiHEPE and 7(*S*),17(*S*)-DiHDHA and (ii) a mixture of 5(*R/S*),15(*S*)-DiHETE, 5(*R/S*),15(*S*)-DiHEPE and 7(*R/S*),17(*S*)-DiHDHA, which was generated by conversion of 5(*R,S*)-HETE, 5(*R,S*)-HEPE and 7(*R,S*)-HDHA by human 15-LOX. **B:** ²D chromatograms (MRM signals) following chiral separation of (i) 5,15-DiHETE, 5,15-DiHEPE and 7,17-DiHDHA derived from enantiopure reference standards, (ii) enzymatically formed diastereomers, (iii) oxidized (commercial) human plasma and (iv) human M2-like macrophages. **C:** Exemplary identical MS² spectra of the four stereoisomers of 5,15-DiHETE from oxidized human plasma and structure of the oxylipin indicating suggested sites of fragmentation leading to the fragment ions. The following MRM transitions were used: 5,15-DiHETE: m/z 335→173; 5,15-DiHEPE: m/z 333→173; 7,17-DiHDHA: m/z 359→141. *: Stereo configuration of these isomers is estimated based on elution order.

docosahexaenoic acid (protectin DX) and its 10(*R*),17(*S*)-diastereomer (supplemental Fig. S9).

Following heart-cutting and chiral chromatography, baseline separation of all diastereomers was achieved, and stereo information could be assigned by comparison with the enantiopure reference standard (Fig. 6B). Chiral analysis following heart-cutting of 5,15-DiHETE from all oxidized plasmas yielded four peaks (Fig. 6B) showing the exactly same MS² spectra (Fig. 6C). Based on the identical retention times of the enzymatically generated standards, two peaks were identified as 5(*R*),15(*S*)- and 5(*S*),15(*S*)-DiHETE. The two other peaks were assigned to the corresponding enantiomers, assuming, based on the general earlier retention time of *R*-hydroxy-FA, that the (*R*),(*R*) isomer elutes first. Following ²D chiral analysis of 5,15-DiHEPE and 7,17-DiHDHA from oxidized plasma, three peaks are detected, with one peak being twice as high as the others (Fig. 6B). It can be assumed that two of the four stereoisomers are coeluting. Based on the retention time and peak height presumably 5(*R*),15(*S*)- and 5(*S*),15(*R*)-DiHEPE as well as 7(*R*),17(*S*)- and 7(*S*),17(*R*)-DiHDHA elute together (Fig. 6B). The stereoisomers resulting from the catalytic activities of 5-LOX and 15-LOX, ie bearing (*S,S*) configuration of the hydroxy groups, are thus baseline-separated from their enantiomer and diastereomers. This allows us to distinguish it from non-enzymatically formed oxidation products. The occurrence of all four stereoisomers in the plasma confirms the autooxidative origin of 5,15-DiHEPE, 5,15-DiHETE, and 7,17-DiHDHA in all investigated plasma samples.

To analyze an enzymatic formation of dihydroxy-FA, human M2-like macrophages derived from human monocytes by differentiation with colony-stimulating factor (CSF) 1 and interleukin (IL) 4 were employed. In these cells, 15-LOX, which gives rise to hydro(pero)xy-FA in *S*-configuration (eg, 12(*S*)- and 15(*S*)-HETE), is highly abundant (3). Consequently, the 15-LOX products 15-HETE, 17-HDHA, and 15-HEPE are present in higher concentrations (~150 pmol/mg protein, ~25 pmol/mg protein, and ~3 pmol/mg protein, respectively), compared with non-esterified 5-HETE, 4-HDHA (both ~2 pmol/mg protein), and 5-HEPE (~0.01 pmol/mg protein). 5,15-DiHEPE, 5,15-DiHETE, and 7,17-DiHDHA were found in concentrations of 20–50 pmol per mg protein (~1.3–3.6 ng per 10⁶ cells), which is in line with the consistent reports about their occurrence in (M2-like) macrophages (53).

MHC-2D-LC-MS/MS revealed that among the stereoisomers, 5(*S*),15(*S*)-DiHETE, 5(*S*),15(*S*)-DiHEPE, and 7(*S*),17(*S*)-DiHDHA are dominantly found. The (*R,R*)-enantiomers were not detected, and only negligible amounts of the (*S,R*)- and (*R,S*)-diastereomers were present (Fig. 6B). This result demonstrates that 5,15-DiHETE, 5,15-DiHEPE, and 7,17-DiHDHA in human M2-like macrophages are of enzymatic origin and are indeed 5(*S*),15(*S*)-DiHETE, resolvin E4, and resolvin D5.

The fact that only the (*S,S*) enantiomer is detected supports the assumption of their formation by consecutive LOX-catalyzed reactions (48, 53), removal of the 5(*R*) or 7(*R*)-hydroxy-FA (59), or a preference of the 15-LOX for the 5(*S*)- or 7(*S*)-hydroxy-FA substrate. However, the functional physiological relevance of the macrophages' capacity to form these SPMs remains to be clarified (48, 52).


For 10,17-DiHDHA, two stereoisomers, that is, 10(*S*),17(*S*)-DiHDHA ("protectin DX") and 10(*R*),17(*S*)-DiHDHA, are detected in macrophages, since only the oxidation at position 17 is enzymatically catalyzed (by 15-LOX), whereas the oxidation at position 10 is not (supplemental Fig. S9) (59). It is postulated that the 17(*S*)-hydroperoxy-DHA eg formed by 15-LOX, can be converted to 10(*R*),17(*S*)-DiHDHA with an (*E,E,Z*)-configured triene system ("neuroprotectin D1") (60–62). ²D chiral analysis of the presumptive peak of "neuroprotection D1" revealed that the single peak detected following RP chromatography consists of at least three isomers of which neuroprotectin D1 is not the major component (supplemental Fig. S9). It can therefore be assumed that this 10,17-DiHDHA is not formed by controlled enzymatic reactions, and the suggested formation of neuroprotectin D1 does not occur in human M2-like macrophages. Several 10,17-DiHDHA isomers, but not neuroprotectin D1, have been found following enzyme incubations in vitro (61) and in plasma stored for a long time at –20°C by chiral chromatography (49). It is therefore unlikely that neuroprotectin D1 occurs in biological samples in relevant amounts compared with its isomers.

Several chiral LC methods have been used for SPM analysis (11, 39, 49, 63), but the stereo configuration of 5(*S*),15(*S*)-DiHETE, 5(*S*),15(*S*)-DiHEPE (resolvin E4) and 7(*S*),17(*S*)-DiHDHA (resolvin D5) has not been comprehensively analyzed in biological samples. Here, we demonstrate that RP chromatography not only leads to the expected co-elution of their enantiomers but also of the diastereomers. Thus, if chromatography without a chiral selector is performed, all stereoisomers in sum are determined, and not one specific isomer of the lipid. Indeed, 5(*S*),15(*S*)-DiHEPE (resolvin E4) and 7(*S*),17(*S*)-DiHDHA (resolvin D5) are present in human M2-like macrophages. However, in other biological samples, all four isomers of the dihydroxy-FA can occur, as demonstrated for oxidized plasma (Fig. 6B). Reporting 5,15-DiHEPE and 7,17-DiHDHA as resolvins E4 and D5, respectively, following achiral RP chromatography is therefore misleading. Only chiral separation as developed here allows to demonstrate the presence of 5(*S*),15(*S*)-DiHEPE (resolvin E4) and 7(*S*),17(*S*)-DiHDHA (resolvin D5) in biological samples.

The developed MHC-2D-LC-MS/MS method is, therefore, an important tool for the separation of both, enantiomeric, and diastereomeric oxylipins. With that, the stereoconfiguration can be unveiled enabling a better characterization of the oxylipins found in

biological samples and their formation pathways. This method is the first combination of targeted oxylipin metabolomics and enantioselective analysis in two-dimensional LC. This new dimension of oxylipin analysis can be readily used to extend existing LC-MS/MS oxylipin platforms. Clinical samples can be analyzed for enantiomeric ratios from the same sample without the need for additional sample preparation steps or additional sample materials. Owing this the method paves the route for gaining new insights into the pathways of oxylipin formation in biological samples, leading to a better understanding of their role in physiological processes.

Data availability

All data are contained within the article or supplementary material. 

Supplemental Data

This article contains [Supplemental Data](#) (3, 10, 12–16, 21, 32–34, 49, 54, 61, 64–73).

Acknowledgment

This work was supported by a Ph.D. scholarship from the Friedrich-Ebert-Stiftung e.V. to R. K.

Author contributions

A. L., R. K., N. H. S., and N. K. writing–review & editing; A. L., R. K., and N. K. investigation; A. L., R. K., and N. K. formal analysis; N. H. S. and N. K. writing–original draft; N. H. S. resources; N. H. S. and N. K. methodology.

Author ORCIDs

Nadja Kampschulte  <https://orcid.org/0000-0002-6253-9939>

Rebecca Kirchhoff  <https://orcid.org/0009-0003-7196-9943>

Ariane Löwen  <https://orcid.org/0009-0000-4590-567X>

Nils Helge Schebb  <https://orcid.org/0000-0003-1299-6629>

Funding and additional information

Our work is supported by a grant (SCHE 1801) from the German Research Foundation to N. H. S.

Conflict of interests

The authors declare that they have no conflicts of interest with the contents of this article.

Abbreviations

¹D, first dimension; ²D, second dimension; ARA, arachidonic acid; ASA, acetylsalicylic acid; ASM, active solvent modulation; CYP, cytochrome P450 monooxygenase; COX, cyclooxygenase; DHA, docosahexanoic acid; DiHDHA, dihydroxydocosahexanoic acid; DiHDPE, dihydroxydocosapentaenoic acid; DiHEPE, dihydroxyeicosapentaenoic acid; DiHETE, dihydroxyeicosatetraenoic acid; DiHETrE, dihydroxyeicosatrienoic acid; DiHODE, dihydroxyoctadecenoic acid; DiHOME, dihydroxyoctadecenoic acid; EF, enantiomeric fraction; EPA, eicosapentaenoic acid; FA, fatty acid; HDHA,

hydroxydocosahexanoic acid; HEPE, hydroxyeicosapentaenoic acid; HETE, hydroxyeicosatetraenoic acid; HODE, hydroxyoctadecenoic acid; HOTrE, hydroxyoctatrienoic acid; LOX, lipoxygenase; MHC, multiple heart-cutting; NP, normal phase; RP, reversed-phase; *t*BuOOH, *tert*-butyl hydroperoxide.

Manuscript received September 13, 2024, and in revised form October 28, 2024. Published, JLR Papers in Press, November 5, 2024, <https://doi.org/10.1016/j.jlr.2024.100694>

REFERENCES

- Gabbs, M., Leng, S., Devassy, J. G., Monirujjaman, M., and Aukema, H. M. (2015) Advances in our understanding of oxylipins derived from dietary PUFAs. *Adv. Nutr.* **6**, 513–540
- Buczynski, M. W., Dumlao, D. S., and Dennis, E. A. (2009) Thematic Review Series: proteomics. An integrated omics analysis of eicosanoid biology[S]. *J. Lipid Res.* **50**, 1015–1038
- Hartung, N. M., Mainka, M., Pfaff, R., Kuhn, M., Biernacki, S., Zinnert, L., *et al.* (2023) Development of a quantitative proteomics approach for cyclooxygenases and lipoxygenases in parallel to quantitative oxylipin analysis allowing the comprehensive investigation of the arachidonic acid cascade. *Anal. Bioanal. Chem.* **415**, 913–933
- Dumlao, D. S., Buczynski, M. W., Norris, P. C., Harkewicz, R., and Dennis, E. A. (2011) High-throughput lipidomic analysis of fatty acid derived eicosanoids and N-acyl ethanolamines. *Biochim. Biophys. Acta (Bba) - Mol. Cell Biol. Lipids.* **1811**, 724–736
- Berkecz, R., Lísá, M., and Holčápek, M. (2017) Analysis of oxylipins in human plasma: comparison of ultrahigh-performance liquid chromatography and ultrahigh-performance supercritical fluid chromatography coupled to mass spectrometry. *J. Chromatogr. A.* **1511**, 107–121
- Chen, G.-y., and Zhang, Q. (2019) Comprehensive analysis of oxylipins in human plasma using reversed-phase liquid chromatography-triple quadrupole mass spectrometry with heatmap-assisted selection of transitions. *Anal. Bioanal. Chem.* **411**, 367–385
- Pedersen, T. L., Gray, I. J., and Newman, J. W. (2021) Plasma and serum oxylipin, endocannabinoid, bile acid, steroid, fatty acid and nonsteroidal anti-inflammatory drug quantification in a 96-well plate format. *Analytica Chim. Acta.* **1143**, 189–200
- Powell, W. S., and Rokach, J. (2015) Biosynthesis, biological effects, and receptors of hydroxyeicosatetraenoic acids (HETEs) and oxoeicosatetraenoic acids (oxo-ETEs) derived from arachidonic acid. *Biochim. Biophys. Acta (Bba) - Mol. Cell Biol. Lipids.* **1851**, 340–355
- Powell, W. S., Gravelle, F., and Gravel, S. (1992) Metabolism of 5(S)-hydroxy-6,8,11,14-eicosatetraenoic acid and other 5(S)-hydroxyeicosanoids by a specific dehydrogenase in human polymorphonuclear leukocytes. *J. Biol. Chem.* **267**, 19233–19241
- Blum, M., Dogan, I., Karber, M., Rothe, M., and Schunck, W.-H. (2019) Chiral lipidomics of monoepoxy and monohydroxy metabolites derived from long-chain polyunsaturated fatty acids[S]. *J. Lipid Res.* **60**, 135–148
- Toewe, A., Balas, L., Durand, T., Geisslinger, G., and Ferreirós, N. (2018) Simultaneous determination of PUFA-derived pro-resolving metabolites and pathway markers using chiral chromatography and tandem mass spectrometry. *Analytica Chim. Acta.* **1031**, 185–194
- Cebo, M., Fu, X., Gawaz, M., Chatterjee, M., and Lämmerhofer, M. (2020) Enantioselective ultra-high performance liquid chromatography-tandem mass spectrometry method based on sub-2-μm particle polysaccharide column for chiral separation of oxylipins and its application for the analysis of autoxidized fatty acids and platelet releasates. *J. Chromatogr. A.* **1624**, 461206
- Isse, F. A., Alammari, A. H., El-Sherbeni, A. A., Brocks, D. R., and El-Kadi, A. O. S. (2023) The enantioselective separation and quantitation of the hydroxy-metabolites of arachidonic acid by liquid chromatography – tandem mass spectrometry. *Prostaglandins & Other Lipid Mediators.* **165**, 106701
- Bayer, M., Mosandl, A., and Thaçi, D. (2005) Improved enantioselective analysis of polyunsaturated hydroxy fatty acids in

- psoriatic skin scales using high-performance liquid chromatography. *J. Chromatogr. B* **819**, 323–328
15. Schneider, C., Yu, Z., Boeglin, W. E., Zheng, Y., and Brash, A. R. (2007) Enantiomeric separation of hydroxy and hydroperoxy eicosanoids by chiral column chromatography. In *27. Methods in Enzymology*. Academic Press, 145–157
 16. Quaranta, A., Zöhrer, B., Revol-Cavalier, J., Benkestock, K., Balas, L., Oger, C., *et al.* (2022) Development of a chiral supercritical fluid chromatography–tandem mass spectrometry and reversed-phase liquid chromatography–tandem mass spectrometry platform for the quantitative metabolic profiling of octadecanoid oxylipins. *Anal. Chem.* **94**, 14618–14626
 17. Serhan, C. N., Yang, R., Martinod, K., Kasuga, K., Pillai, P. S., Porter, T. F., *et al.* (2008) Maresins: novel macrophage mediators with potent antiinflammatory and proresolving actions. *J. Exp. Med.* **206**, 15–23
 18. Schneider, C., Boeglin, W. E., and Brash, A. R. (2000) Enantiomeric separation of hydroxy eicosanoids by chiral column chromatography: effect of the alcohol modifier. *Anal. Biochem.* **287**, 186–189
 19. Mazaleuskaya, L. L., Salamatipour, A., Sarantopoulou, D., Weng, L., FitzGerald, G. A., Blair, I. A., *et al.* (2018) Analysis of HETEs in human whole blood by chiral UHPLC-ECAPCI/HRMS. *J. Lipid Res.* **59**, 564–575
 20. Tacconelli, S., Fullone, R., Dovizio, M., Pizzicoli, G., Marschler, S., Bruno, A., *et al.* (2020) Pharmacological characterization of the biosynthesis of prostanooids and hydroxyeicosatetraenoic acids in human whole blood and platelets by targeted chiral lipidomics analysis. *Biochim. Biophys. Acta (Bba) - Mol. Cell Biol. Lipids.* **1865**, 158804
 21. Fu, X., Xu, Z., Gawaz, M., and Lämmerhofer, M. (2023) UHPLC-MS/MS method for chiral separation of 3-hydroxy fatty acids on amylose-based chiral stationary phase and its application for the enantioselective analysis in plasma and platelets. *J. Pharm. Biomed. Anal.* **223**, 115151
 22. Gladine, C., Ostermann, A. I., Newman, J. W., and Schebb, N. H. (2019) MS-based targeted metabolomics of eicosanoids and other oxylipins: analytical and inter-individual variabilities. *Free Radic. Biol. Med.* **144**, 72–89
 23. Guillén-Casla, V., León-González, M. E., Pérez-Arribas, L. V., and Polo-Díez, L. M. (2010) Direct chiral determination of free amino acid enantiomers by two-dimensional liquid chromatography: application to control transformations in E-beam irradiated foodstuffs. *Anal. Bioanal. Chem.* **397**, 63–75
 24. Karongo, R., Ge, M., Geibel, C., Horak, J., and Lämmerhofer, M. (2021) Enantioselective multiple heart cutting online two-dimensional liquid chromatography-mass spectrometry of all proteinogenic amino acids with second dimension chiral separations in one-minute time scales on a chiral tandem column. *Analytica Chim. Acta* **1180**, 338858
 25. Yang, Y., Rosales-Conrado, N., Guillén-Casla, V., León-González, M. E., Pérez-Arribas, L. V., and Polo-Díez, L. M. (2012) Chiral determination of salbutamol, salmeterol and atenolol by two-dimensional LC-LC: application to urine samples. *Chromatographia* **75**, 1365–1375
 26. Peñín-Ibáñez, M., Santos-Delgado, M. J., and Polo-Díez, L. M. (2018) Determination of profens in pharmaceuticals by heart-cut achiral-chiral two-dimensional HPLC. *Separation Science Plus* **1**, 168–176
 27. Pursch, M., and Buckenmaier, S. (2015) Loop-based multiple heart-cutting two-dimensional liquid chromatography for target analysis in complex matrices. *Anal. Chem.* **87**, 5310–5317
 28. Rund, K. M., Ostermann, A. I., Kutzner, L., Galano, J.-M., Oger, C., Vigor, C., *et al.* (2018) Development of an LC-ESI(-)MS/MS method for the simultaneous quantification of 35 isoprostanes and isofurans derived from the major n3- and n6-PUFAs. *Analytica Chim. Acta* **1037**, 63–74
 29. Willenberg, I., Meschede, A. K., and Schebb, N. H. (2015) Determining cyclooxygenase-2 activity in three different test systems utilizing online-solid phase extraction-liquid chromatography-mass spectrometry for parallel quantification of prostaglandin E2, D2 and thromboxane B2. *J. Chromatogr. A* **1391**, 40–48
 30. Goebel, B., Carpanedo, L., Reif, S., Göbel, T., Simonyi, S., Schebb, N. H., *et al.* (2023) Development of a cell-based model system for the investigation of ferroptosis. *Front. Cell Death* **2**. <https://doi.org/10.3389/fceld.2023.1182239>
 31. Ebert, R., Cumbana, R., Lehmann, C., Kutzner, L., Toewe, A., Ferreirós, N., *et al.* (2020) Long-term stimulation of toll-like receptor-2 and -4 upregulates 5-LO and 15-LO-2 expression thereby inducing a lipid mediator shift in human monocyte-derived macrophages. *Biochim. Biophys. Acta (Bba) - Mol. Cell Biol. Lipids.* **1865**, 158702
 32. Jüßermann, M. (2018) Totalsynthese von 18-HEPE und unnatürlichen Hydroxy-PUFAs. Bergische Universität Wuppertal, Wuppertal (online). [urn:nbn:de:hbz:468-20180815-111539-1](https://nbn-resolving.org/urn:nbn:de:hbz:468-20180815-111539-1)
 33. Kutzner, L., Rund, K. M., Ostermann, A. I., Hartung, N. M., Galano, J.-M., Balas, L., *et al.* (2019) Development of an optimized LC-MS method for the detection of specialized pro-resolving mediators in biological samples. *Front. Pharmacol.* **10**, 169
 34. Koch, E., Mainka, M., Dalle, C., Ostermann, A. I., Rund, K. M., Kutzner, L., *et al.* (2020) Stability of oxylipins during plasma generation and long-term storage. *Talanta* **217**, 121074
 35. Lee, S. H., Williams, M. V., DuBois, R. N., and Blair, I. A. (2003) Targeted lipidomics using electron capture atmospheric pressure chemical ionization mass spectrometry. *Rapid Commun. Mass Spectrom.* **17**, 2168–2176
 36. Li, F., Su, X., Bäurer, S., and Lämmerhofer, M. (2020) Multiple heart-cutting mixed-mode chromatography-reversed-phase 2D-liquid chromatography method for separation and mass spectrometric characterization of synthetic oligonucleotides. *J. Chromatogr. A* **1625**, 461338
 37. van de Schans, M. G. M., Blokland, M. H., Zoontjes, P. W., Mulder, P. P. J., and Nielen, M. W. F. (2017) Multiple heart-cutting two dimensional liquid chromatography quadrupole time-of-flight mass spectrometry of pyrrolizidine alkaloids. *J. Chromatogr. A* **1503**, 38–48
 38. Koga, R., Miyoshi, Y., Negishi, E., Kaneko, T., Mita, M., Lindner, W., *et al.* (2012) Enantioselective two-dimensional high-performance liquid chromatographic determination of N-methyl-D-aspartic acid and its analogues in mammals and bivalves. *J. Chromatogr. A* **1269**, 255–261
 39. Oh, S. F., Vickery, T. W., and Serhan, C. N. (2011) Chiral lipidomics of E-series resolvins: aspirin and the biosynthesis of novel mediators. *Biochim. Biophys. Acta (Bba) - Mol. Cell Biol. Lipids.* **1811**, 737–747
 40. Tiritan, M. E., Fernandes, C., Maia, A. S., Pinto, M., and Cass, Q. B. (2018) Enantiomeric ratios: why so many notations? *J. Chromatogr. A* **1569**, 1–7
 41. Ostermann, A. I., Koch, E., Rund, K. M., Kutzner, L., Mainka, M., and Schebb, N. H. (2020) Targeting esterified oxylipins by LC-MS - effect of sample preparation on oxylipin pattern. *Prostaglandins & Other Lipid Mediators* **146**, 106384
 42. Hartung, N. M., Mainka, M., Kampschulte, N., Ostermann, A. I., and Schebb, N. H. (2019) A strategy for validating concentrations of oxylipin standards for external calibration. *Prostaglandins & Other Lipid Mediators* **141**, 22–24
 43. Ostermann, A. I., Willenberg, I., and Schebb, N. H. (2015) Comparison of sample preparation methods for the quantitative analysis of eicosanoids and other oxylipins in plasma by means of LC-MS/MS. *Anal. Bioanal. Chem.* **407**, 1403–1414
 44. Hartung, N. M., Ostermann, A. I., Immenschuh, S., and Schebb, N. H. (2021) Combined targeted proteomics and oxylipin metabolomics for monitoring of the COX-2 pathway. *Proteomics* **21**, 1900058
 45. Thuresson, E. D., Lakkides, K. M., and Smith, W. L. (2000) Different catalytically competent arrangements of arachidonic acid within the cyclooxygenase active site of prostaglandin endoperoxide H synthase-1 lead to the formation of different oxygenated products. *J. Biol. Chem.* **275**, 8501–8507
 46. Giménez-Bastida, J. A., Boeglin, W. E., Boutaud, O., Malkowski, M. G., and Schneider, C. (2019) Residual cyclooxygenase activity of aspirin-acetylated COX-2 forms 15R-prostaglandins that inhibit platelet aggregation. *FASEB J.* **33**, 1033–1041
 47. Lucido, M. J., Orlando, B. J., Vecchio, A. J., and Malkowski, M. G. (2016) Crystal structure of aspirin-acetylated human cyclooxygenase-2: insight into the formation of products with reversed stereochemistry. *Biochemistry* **55**, 1226–1238
 48. Schebb, N. H., Kühn, H., Kahnt, A. S., Rund, K. M., O'Donnell, V. B., Flamand, N., *et al.* (2022) Formation, signaling and occurrence of specialized pro-resolving lipid mediators—what is the evidence so far? *Front. Pharmacol.* **13**, 838782
 49. Jonasdottir, H. S., Brouwers, H., Toes, R. E. M., Ioan-Facsinay, A., and Giera, M. (2018) Effects of anticoagulants and storage conditions on clinical oxylipid levels in human plasma. *Biochim. Biophys. Acta (Bba) - Mol. Cell Biol. Lipids.* **1863**, 1511–1522

50. Morisseau, C., and Hammock, B. D. (2013) Impact of soluble epoxide hydrolase and epoxyeicosanoids on human health. *Annu. Rev. Pharmacol. Toxicol.* **53**, 37–58
51. Ikei, K. N., Yeung, J., Apopa, P. L., Ceja, J., Vesci, J., Holman, T. R., *et al.* (2012) Investigations of human platelet-type 12-lipoxygenase: role of lipoxygenase products in platelet activation[S]. *J. Lipid Res.* **53**, 2546–2559
52. Alnouri, M. W., Roquid, K. A., Bonnavion, R., Cho, H., Heering, J., Kwon, J., *et al.* (2024) SPMs exert anti-inflammatory and pro-resolving effects through positive allosteric modulation of the prostaglandin EP4 receptor. *Proc. Natl. Acad. Sci.* **121**, e2407130121
53. Kahnt, A. S., Schebb, N. H., and Steinhilber, D. (2023) Formation of lipoxins and resolvins in human leukocytes. *Prostaglandins & Other Lipid Mediators.* **166**, 106726
54. Kutzner, L., Goloschapova, K., Rund, K. M., Jubermaun, M., Blum, M., Rothe, M., *et al.* (2020) Human lipoxygenase isoforms form complex patterns of double and triple oxygenated compounds from eicosapentaenoic acid. *Biochim. Biophys. Acta Mol. Cell Biol. Lipids.* **1865**, 158806
55. Mainka, M., George, S., Angioni, C., Ebert, R., Goebel, T., Kampschulte, N., *et al.* (2022) On the biosynthesis of specialized pro-resolving mediators in human neutrophils and the influence of cell integrity. *Biochim. Biophys. Acta (Bba) - Mol. Cell Biol. Lipids.* **1867**, 159093
56. Colas, R. A., Shinohara, M., Dalli, J., Chiang, N., and Serhan, C. N. (2014) Identification and signature profiles for pro-resolving and inflammatory lipid mediators in human tissue. *Am. J. Physiology-Cell Physiol.* **307**, C39–C54
57. Skarke, C., Alamuddin, N., Lawson, J. A., Li, X., Ferguson, J. F., Reilly, M. P., *et al.* (2015) Bioactive products formed in humans from fish oils. *J. Lipid Res.* **56**, 1808–1820
58. Kühn, H., Barnett, J., Grunberger, D., Baecker, P., Chow, J., Nguyen, B., *et al.* (1993) Overexpression, purification and characterization of human recombinant 15-lipoxygenase. *Biochim. Biophys. Acta (Bba) - Lipids Lipid Metab.* **1169**, 80–89
59. Kirchhoff, R., Kampschulte, N., Rothweiler, C., Rohwer, N., Weylandt, K.-H., and Schebb, N. H. (2024) An optimized *ex vivo* n-3 PUFA supplementation strategy for primary human macrophages shows that DHA suppresses prostaglandin E2 formation. *Mol. Nutr. Food Res.* <https://doi.org/10.1002/mnfr.202400716> R1
60. Stenvik Haatveit, Å., and Hansen, T. V. (2023) The biosynthetic pathways of the protectins. *Prostaglandins & Other Lipid Mediators.* **169**, 106787
61. Jin, J., Boeglin, W. E., and Brash, A. R. (2021) Analysis of 12/15-lipoxygenase metabolism of EPA and DHA with special attention to authentication of docosatrienes. *J. Lipid Res.* **62**, 100088
62. Serhan, C. N., Gotlinger, K., Hong, S., Lu, Y., Siegelman, J., Baer, T., *et al.* (2006) Anti-inflammatory actions of neuroprotectin D1/protectin D1 and its natural stereoisomers: assignments of dihydroxy-containing docosatrienes. *J. Immunol.* **176**, 1848–1859
63. Homann, J., Lehmann, C., Kahnt, A. S., Steinhilber, D., Parnham, M. J., Geisslinger, G., *et al.* (2014) Chiral chromatography–tandem mass spectrometry applied to the determination of pro-resolving lipid mediators. *J. Chromatogr. A.* **1360**, 150–163
64. Capdevila, J. H., Wei, S., Kumar, A., Kobayashi, J., Snapper, J. R., Zeldin, D. C., *et al.* (1992) Resolution of dihydroxyeicosanoates and of dihydroxyeicosatrienoates by chiral phase chromatography. *Anal. Biochem.* **207**, 236–240
65. Koch, E., and Kampschulte, N. (2022) Comprehensive analysis of fatty acid and oxylipin patterns in n3-PUFA supplements. *J. Agri. Food Chem.* **70**, 3979–3988
66. Pursch, M., and Wegener, A. (2018) Evaluation of active solvent modulation to enhance two-dimensional liquid chromatography for target analysis in polymeric matrices. *J. Chromatogr. A.* **1562**, 78–86
67. Stoll, D. R., Shoykhet, K., and Petersson, P. (2017) Active solvent modulation: a valve-based approach to improve separation compatibility in two-dimensional liquid chromatography. *Anal. Chem.* **89**, 9260–9267
68. Pardon, M., Chapel, S., and de Witte, P. (2023) Optimizing transfer and dilution processes when using active solvent modulation in on-line two-dimensional liquid chromatography. *Anal. Chim. Acta.* **1252**, 341040
69. Bäurer, S., Guo, W., and Polnick, S. (2019) Simultaneous separation of water- and fat-soluble vitamins by selective comprehensive HILIC × RPLC (high-resolution sampling) and active solvent modulation. *Chromatographia.* **82**, 167–180
70. Caño-Carrillo, I., Martínez-Piarnas, A. B., Gilbert-López, B., Molina-Díaz, A., and García-Reyes, J. F. (2024) Simultaneous analysis of highly polar and multi-residue-type pesticides by heart-cutting 2D-LC-MS. *Talanta.* **266**, 124918
71. Chen, P., Fenet, B., Michaud, S., Tomczyk, N., Véricel, E., and Lagarde, M. (2009) Full characterization of PDX, a neuroprotectin/protectin D1 isomer, which inhibits blood platelet aggregation. *FEBS Lett.* **583**, 3478–3484
72. Balas, L., Guichardant, M., and Durand, T. (2014) Confusion between protectin D1 (PD1) and its isomer protectin DX (PDX). An overview on the dihydroxy-docosatrienes described to date. *Biochimie.* **99**, 1–7
73. Rund, K. M., Peng, S., Greite, R., Claaßen, C., Nolte, F., Oger, C., *et al.* (2020) Dietary omega-3 PUFA improved tubular function after ischemia induced acute kidney injury in mice but did not attenuate impairment of renal function, *Prostaglandins & Other Lipid Mediators.* **146**, 106386